Desalination and Water Treatment
www.deswater.com
doi: 10.5004/dwt.2020.25748

190 (2020) 267–278
June

Enhanced desorption performance of aniline-saturated powdered activated carbon using ultrasound assisted with ethanol

Rui Yu, Xing Li, Yanling Yang, Tingting Zhang, Zhiwei Zhou*

College of Architecture and Civil engineering, Beijing University of Technology, Beijing 100124, China, Tel. +86 10 67391726; emails: hubeizhouzhiwei@163.com (Z. Zhou), 1571073955@qq.com (R. Yu), lixing@bjut.edu.cn (X. Li), yangyanling@bjut.edu.cn (Y. Yang), zhangting1229ztt@163.com (T. Zhang)

Received 12 August 2019; Accepted 10 February 2020

ABSTRACT

The adsorption characteristics of dissolved aniline onto powdered activated carbon (PAC) and the subsequent desorption by ultrasound treatment were studied. The results indicated that the adsorption followed the pseudo-second-order model and the Langmuir model. Acidic conditions were not conducive to the adsorption of aniline. The desorption efficiency of saturated PAC radiated by ultrasound reached a maximum of 24.35% with a sonication power of 180 W at a frequency of 40 kHz, and a pH of 3 within 180 min of sonication time. The addition of ethanol produced a synergistic effect with ultrasound, effectively improved the desorption efficiency to 83.88%. Intermediates of aniline that were formed during the ultrasound irradiation were analyzed by gas chromatography-mass spectrometry and this identified azobenzene as the main by-product. Analysis of the specific surface area, pore structure, and FTIR spectra of PAC indicated that more cavitation occurred in ethanol than in water, and high-speed microjets and high-pressure microstreams enlarged the mesopore of PAC. In general, the physical attack of microjets and microstreams played an active role in the desorption of aniline.

Keywords: Aniline; Powdered activated carbon; Ultrasound; Adsorption; Desorption

1. Introduction

Aniline is an important industrial ingredient used for printing, dyeing, pesticide production, rubber additives and other applications. It is widely present in the industrial wastewater from production facilities of pesticides, dyes and petrochemicals [1,2]. Due to its high solubility and noted hepatic toxicity, it is harmful even at low concentrations in an aquatic environment [3]. Therefore, wastewater effluent containing aniline should be cautiously treated before released into the environment.

Many studies have addressed the removal of aniline from wastewater using various treatments such as degradation [4], biodegradation [5], electrolysis [6], and adsorption [7]. Among all these approaches, adsorption using activated carbon is most often applied to remove aniline because this adsorbent has a high specific surface area and a suitable pore structure [8]. However, when the activated carbon is saturated, it is often incinerated or discarded, which limited its application severely. Regeneration of used activated carbon is necessary to reduce costs, enable re-use, and avoid secondary pollution [9].

Common techniques for regeneration of activated carbon include thermal regeneration [10], electrochemical regeneration [11], biodegradation [12], solvent regeneration [13], and microwave irradiation [14]. In addition, ultrasonic technology is a new technology that is environmentally friendly and has low energy consumption. Ultrasound has been applied to the regeneration of activated carbon

* Corresponding author.

saturated with phenol [15], chlorophenol [16], trihalomethane [17] and other pollutants. Ultrasonic treatment can disturb the physical bonds between adsorbate and adsorbent by two major mechanisms. On the one hand, free radicals are generated during cavitation, which can directly degrade organic matter, as has been demonstrated for dyes [18], aromatic hydrocarbons [19] and pesticides [20]. On the other hand, the cavitation bubbles generated by ultrasound can reach nuclear temperatures of 5,000 K and pressures of 5.05×10^7 upon collapse, and these extreme conditions, that last for nanoseconds to microseconds, are accompanied by shock waves and high-speed microjets that detach the adsorbent from the adsorbate [21]. Aniline is a semi-volatile aromatic compound with a low boiling point that volatilizes at elevated temperatures. When using ultrasonic regeneration of activated carbon saturated with aniline, the instantaneous high temperature and high pressure generated by ultrasonic waves may cause aniline volatilization and pyrolysis, which would destroy the compound. In addition, the free radicals generated by cavitation may degrade the adsorbate on the activated carbon and in solution. We therefore expect the physical and chemical effects of ultrasonic treatment to enable desorption of semi-volatile aniline from powdered activated carbon (PAC), for which we explored the efficacy and mechanisms.

In this study, PAC was used to adsorb dissolved aniline and reach its saturation, after which it was subjected to ultrasonic desorption. The detailed objectives were as follows: (1) to investigate the adsorption characteristics of aniline onto PAC; (2) to determine the appropriate desorption conditions including the optimal ultrasonic power and frequency, pH, and ethanol concentration in the solvent; (3) to investigate any synergistic effect of ultrasound and ethanol; (4) to study the mechanism of ultrasonic desorption, to further understand the effect of high-speed microjets, high-pressure shock waves and hydroxyl radicals generated by ultrasound during desorption. The significance of this study was to identify the regeneration performance and mechanism of PAC saturated with aniline under ultrasound treatment.

2. Materials and methods

2.1. Chemicals and instruments

Aniline (purity ≥ 99.5%) and *n*-butanol (purity ≥ 99%) were supplied by Aladdin (Shanghai, China). NaOH, HCl, anhydrous ethanol, and acetic acid at analytical grade were purchased from Beijing Chemical Works (Beijing, China), and used without further purification. All solutions were prepared with ultra-pure water obtained using a Milli-Q Heal Force ultra-pure system.

The characteristics of the PAC used in the experiment are as follows: iodine value 705.80 mg/g, methylene blue adsorption 174.71 mg/g, specific surface area 623.51 m^2/g, average pore diameter 2.80 nm, micropore volume 0.10 cm^3/g and mesopore volume 0.36 cm^3/g. Before use, the PAC was washed and boiled with deionized water three times to remove any soluble impurities. The washed carbon was separated by a 0.45 μm microfiltration membrane, dried at room temperature to a constant weight, and placed in a desiccator for later use.

The desorption and degradation experiments were carried out in a custom ultrasonic cleaner (Kunshan Ultrasonic Instrument Co., Ltd., China) with a frequency range of 20–100 kHz and output power of 20–200 W. In order to maintain the temperature of the reaction, a condenser tube was placed in the ultrasonic bath. The temperature of the solution was maintained at 298 ± 2 K by adjusting the temperature control system of the ultrasonic cleaner and the temperature of the condenser. A cantilever stirrer (Ika Works Guangzhou, China) was used to stir at 150 rpm during all experiments.

2.2. Experimental procedure

2.2.1. Adsorption procedure

For standard adsorption experiments, 250 mL of 100 mg/L aniline dissolved in water was added to a 250 mL conical flask containing dry PAC to give a suspension of 1 g/L. The pH of the solution was adjusted by sodium hydroxide and hydrochloric acid to 7.0 unless stated otherwise, and the flasks were placed in an incubator shaker at 150 rpm at a constant temperature of 298 K. Samples were collected at time intervals from 0 to 270 min and these were filtered with a 0.45 μm regenerated cellulose filter. The amount of aniline in the filtrate was then determined as described below.

For adsorption kinetics, the PAC concentration was varied from 1.0 to 2.0 g/L. For isotherm experiments, the dosage of PAC was varied from 0.2–2.0 g/L and incubation was performed at three different temperatures (298, 308, and 318 K). The incubation was extended to 24 h to assure that adsorption equilibrium was reached.

Batch adsorption experiments were conducted to quantify the factors affecting adsorption. These included the pH, initial aniline concentration, PAC dose, and contact time. The initial pH was adjusted from 3.0 to 11.0 with diluted 0.1 M NaOH or 0.1 M HCl. The influence of aniline concentration was tested for a range of 50–300 mg/L and the PAC dose was varied from 0.5–3 g/L. The effect of contact time was investigated with 1 g/L PAC and variable concentrations of aniline in the range of 50–300 mg/L.

The adsorption capacity of aniline q (mg/g) was calculated by Eq. (1):

$$q = \frac{\left(C_0 - C_t\right)V}{W} \tag{1}$$

where C_0 (mg/L) and C_t are the initial and instant concentration of aniline at time t, V (L) is the volume of the solution, W (g) is the dosage of PAC.

2.2.2. Desorption procedure

Aniline-saturated PAC was prepared under the standard conditions described above, with the exception that adsorption was allowed for 24 h. It was confirmed that at 298 K aniline volatilization was negligible by a blank experiment (no addition of PAC). After the adsorption had reached equilibrium, the saturated PAC was separated by filtration, dried at room temperature to a constant weight, and placed

in a desiccator for later use, while the adsorption capacity was calculated from the filtrate as described above.

In desorption experiments, 1 g/L of saturated PAC was added to a desorption solution and put into the ultrasonic reactor. The ultrasonic power for desorption treatment was varied from 0–180 W with a frequency of 20–100 kHz with a maximum duration of 180 min. The pH of the desorption solution was varied with diluted 0.1 M NaOH or 0.1 M HCl in the range of 3.0–11.0. The desorption was tested with water, anhydrous ethanol, or ethanol/water mixtures of 25%, 50%, and 75% (V/V) as the solvent. The temperature was controlled at 298 K and samples were taken at predetermined intervals.

Desorption efficiency R (%) was calculated by Eq. (2):

$$R = \frac{C_d V}{q_e m} \times 100\% \quad (2)$$

where q_e (mg/g) is the equilibrium adsorption capacity of PAC, C_d (mg/L) is the concentration of aniline in the regenerated solution, m (g) is the amount of saturated PAC added.

2.2.3. Degradation experiments

For degradation experiments, 50 mg/L aniline was degraded in pure water and anhydrous ethanol without activated carbon, respectively. Ultrasonic condition at the power of 180 W and frequency of 40 kHz. At a controlled pH of 7 and temperature at 298 K. Two radical scavengers, *n*-butanol and acetic acid were added separately at concentrations exceeding the molar concentration of aniline 500 times. The presence of aniline degradation products and intermediates was determined by gas chromatography-mass spectrometry (GC-MS) (GCMS-QP2010 SE; Shimadzu, Japan) as previously described [22].

2.3. Analysis methods

The concentration of aniline was analyzed by a colorimetric method using N-(1-naphthyl) ethylenediamine as the chromogenic agent. The absorbance was measured at 545 nm on a UV-VIS spectrometer (UV-2600; SOPTOP, China). Chemical functional groups were identified using FTIR (V70/Hyperion 1000; Bruker, USA) with a wavenumber scanning range of 400–4,000 cm^{-1}, and a scanning resolution of 4 cm^{-1}. The specific surface area and pore size distribution of the PAC were analyzed using a nitrogen gas adsorption-desorption isotherm method with constant temperature gas adsorption at 77 K (Tristar II 3020M; Micromeritics, USA). The physical morphology of the PAC surface was observed using a scanning electron microscope (JEM-2100F; JEOL, Japan).

3. Results and discussion

3.1. Adsorption characteristics of aniline on PAC

3.1.1. Adsorption kinetics

Kinetics experiments were carried out to determine the rate of aniline removal from water by PAC adsorption. The equilibrium adsorption capacity of the PAC tested at a dosage of 1.0, 1.5, and 2.0 mg/L was 58.03, 44.39, and 33.04 mg/g, respectively. Three kinetics models were used to fit the experimental data and to analyze the adsorption dynamics of aniline. The regression results are listed in Table 1, while the respective linear plots are displayed in Fig. A1.

The pseudo-first-order model did not fit very well (average R^2 = 0.906) while the pseudo-second-order model resulted in an excellent fit (average R^2 = 0.999), suggesting the adsorption kinetics of aniline onto PAC was best described by the pseudo-second-order model which is typical for chemisorption [23].

Additionally, the regression line of the intra-particle diffusion model did not pass through the zero points, indicating that intra-particle diffusion was not the sole rate-limiting step in the sorption process. Two linear lines could be fit into the regression line. A boundary layer diffusion effect led to the first linear section of the graph and an intra-particle diffusion effect was most likely responsible for the second linear section [24,25]. Thus, the adsorption process of aniline could be divided into two steps: boundary layer diffusion and intra-particle diffusion.

3.1.2. Adsorption isotherms

Adsorption isotherm experiments were conducted at 298, 308, and 318 K and after equilibrium was reached, the adsorption data were fitted with the Langmuir, Freundlich and Temkin models. The fits of the isotherm data are presented in Fig. A2 and the regression data of the parameters in each model are listed in Table 2.

It is apparent in Fig. A2 that the Langmuir model fitted better to the data than the models of Freundlich and Temkin, as the R^2 values for the Langmuir model were above 0.99 for all isotherm datasets. These findings indicated that the aniline adsorption onto PAC was limited to monolayer coverage, and the surface was relatively homogeneous [26]. It is also observed that the values of R_L were

Table 1
Adsorption kinetics parameters of aniline onto PAC

	Pseudo-first-order			Pseudo-second-order			Intra-particle diffusion		
m (g/L)	K_1	q_e	R^2	K_2	q_e	R^2	K_d	C	R^2
1.0	0.00686	13.183	0.936	0.00426	58.275	0.999	0.899	44.563	0.952
1.5	0.00283	6.825	0.860	0.01479	50.480	0.999	0.293	46.069	0.907
2.0	0.00283	1.640	0.923	0.01925	44.072	0.999	0.175	41.299	0.963

Table 2
Adsorption isotherm parameters of aniline onto PAC

	Langmuir				Freundlich			Temkin		
T (K)	Q (mg/g)	K (L/mg)	R^2	R_L	K_F (mg/g)	$1/n$	R^2	K_T (L/g)	B (J/mol)	R^2
298	67.613	0.096	0.998	0.094	18.423	0.280	0.986	1.564	12.636	0.995
308	63.291	0.176	0.996	0.054	26.078	0.193	0.961	10.820	8.805	0.947
318	48.948	0.190	0.993	0.050	20.431	0.200	0.815	6.167	7.801	0.809

between 0 and 1, which shown that the aniline molecules were desirably adsorbed onto the PAC adsorbent.

3.1.3. Factors affecting adsorption

The effects of pH, initial aniline concentration, PAC dose, and contact time on adsorption are shown in Fig. A3. It can be observed in Fig. A3a that the adsorption capacity of PAC was reduced at pH 3.0, but it was relatively independent on pH at values >5, where aniline is present in non-ionized forms [8]. The deprotonation of aniline explains the weak adsorption under the strongly acidic condition.

As found in Fig. A3b, with an increasing initial aniline concentration from 50 to 300 mg/L, the PAC adsorption capacity gradually increased from 37.36 to 71.68 mg/g. This can be explained by the driving force of increasing aniline concentration [27]. Furthermore, the adsorption capacity decreased with increasing PAC dose from 0.5 to 3 g/L. Higher concentrations of adsorbent could provide more effective adsorption sites and captured more aniline, which resulted in higher removal efficiency.

As shown in Fig. A3c where contact time was varied, the amount of adsorbed aniline sharply increased during the first 3 min and reached equilibrium at 5 min (for the lowest tested aniline concentration) to 30 min for the highest tested aniline concentration of 300 mg/L. At the initial reaction stage, there were a large number of free sites available with a positive charge on the adsorbent surface. As the reaction progresses, due to the repulsive force between the adsorbed aniline and the aniline in the liquid phase, the remaining free surface positions became more difficult to occupy [28].

3.2. Effects of important parameters on desorption of aniline from saturated PAC

3.2.1. Effect of sonication power

The influence of ultrasonic power on the desorption of aniline from saturated PAC is shown in Fig. 1. The PAC had been saturated with aniline for 24 h, resulting in 70.37 mg/g. The desorption efficiency increased gradually with increasing ultrasonic power from 0 to 180 W. The spontaneous desorption efficiency was 5.45% without ultrasonic treatment. A maximum desorption efficiency of 20.95% was reached when ultrasonic radiation was applied at 180 W for 180 min. As the energy increased, more cavitation occurred, and this caused more aniline to desorb from the PAC. Xing and Feng also reported that increasing ultrasonic power increased the desorption efficiency of contaminants [29].

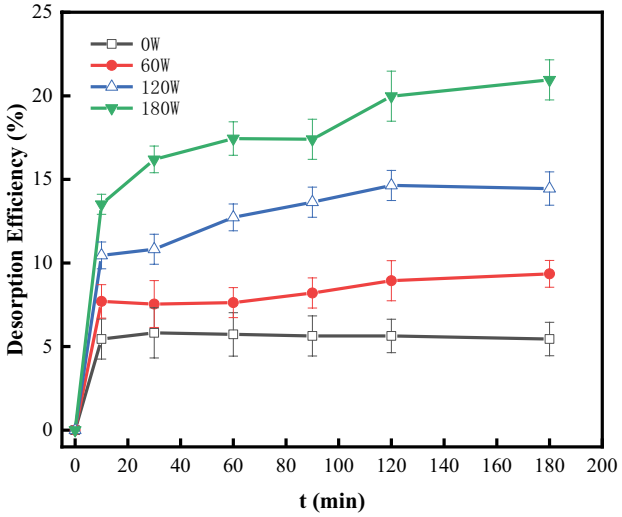

Fig. 1. Effect of ultrasonic power on the desorption efficiency of aniline from saturated PAC. Conditions of desorption: frequency = 40 kHz, T = 298 K, pH = 7.

During the desorption process, ultrasonic waves need to overcome the attraction between aniline and the PAC. With an increase of ultrasonic power, the energy transferred to the system increases and the cavitation effect caused by ultrasound is enhanced, allowing more molecules to break free from the adsorbate [16].

3.2.2. Effect of ultrasonic frequency

The effect of ultrasonic frequency on desorption was also determined (Fig. 2). When the frequency increased from 20 to 40 kHz, the desorption efficiency increased from 7.43% to 20.95%, but higher frequencies resulted in similar or slightly decreased desorption efficiencies. Thus, the frequency of ultrasound affected regeneration and was optimal at 40 kHz, similar results were reported when ultrasound was used to regenerate biologically activated carbon [30]. According to the literature, excessively high ultrasonic frequencies increased the cavitation threshold and released less energy when cavitation bubbles collapsed, resulting in a decrease in desorption efficiency [31]. Theoretically, with an increase of ultrasonic frequency, the acoustic periods shorten, resulting in smaller sized cavitation bubbles, and a shorter collapse duration [32]. Thus, it can be expected that under the action of high frequency, the diameter of bubbles decreases, while micro-jets and micro-streams more effectively act on the small pores of activated carbon, leading to

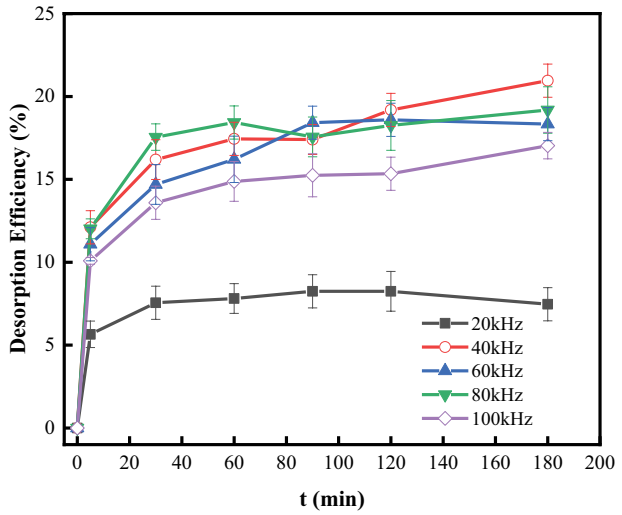

Fig. 2. Effect of ultrasonic frequency on the desorption efficiency of aniline from saturated PAC. Conditions of desorption: power = 180 W, T = 298 K, pH = 7.

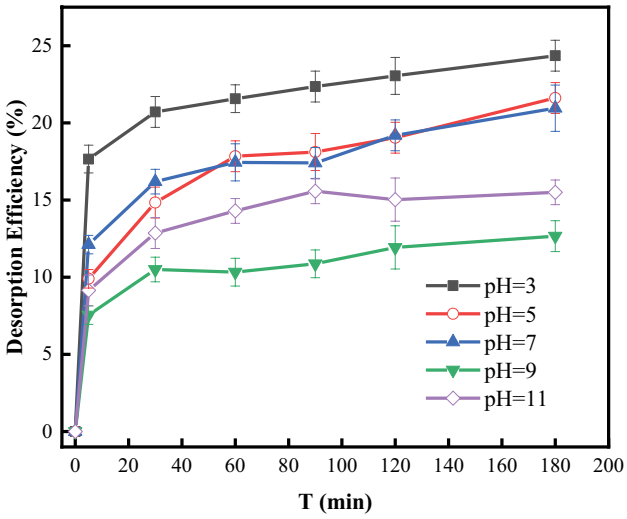

Fig. 3. Effect of initial pH on the desorption efficiency of aniline from saturated PAC. Conditions of desorption: frequency = 40 kHz, power = 180 W, T = 298 K.

improved desorption. However, we discovered this effect was limited to frequencies up to 40 kHz, so presumably the diameter of the produced bubbles was less affected at low frequency, not further improving desorption efficiency.

3.2.3. Effect of pH

The desorption efficiency of aniline under optimal ultrasonic treatment (40 kHz, 180 W) was determined at different pH values and the results are shown in Fig. 3. As expected, the desorption efficiency was highest at a pH of 3, when it reached 24.35%, which was more than double that obtained under alkaline conditions (pH = 11).

The pH of the solution affects the protonation degree of ionizable compounds and functional groups on the adsorbent surface. When the pH of the solution was below 4.6, aniline in solution mainly existed in a positively charged protonated state, while at higher pH the aniline was mainly uncharged [33]. The surface of the PAC carries acid-base functional groups that also present different electrical properties depending on the pH of the solution. At pH 3, the positively-charged aniline was expelled from the positively-charged surface of PAC by electrostatic repulsion. In addition, under acidic conditions the solubility of aniline in water increased, increasing a transition into the aqueous phase. Therefore, ultrasound regeneration of saturated PAC was most effective under acidic conditions. Others have pointed out that pH was an important factor affecting the adsorption of aniline [34], and our findings confirm that pH was also an important factor affecting its desorption.

3.2.4. Effect of addition of ethanol

Aniline is better soluble in organic solvents such as ethanol than in water. Therefore, desorption was tested using a regeneration solution containing increasing amounts of ethanol to see if this improved the transfer of aniline from PAC into the solution. During these experiments, ultrasound was not applied for the first 180 min, after which it was applied at 40 kHz and 180 W for a maximum of 180 min. The results are shown in Fig. 4. During the first 180 min, the presence of 25% (v/v) ethanol significantly promoted the spontaneous transfer of aniline into the liquid phase, increasing the desorption efficiency from 5.45% to 25%. However, higher concentrations of ethanol barely increased this desorption efficiency further. An effect of solvent addition is typically seen when the binding forces between aniline and PAC are weaker than the interaction between the aniline and the solvent. The findings suggested that ethanol promoted desorption of a fraction of the aniline that was bound to PAC with weak forces only, while the remaining fraction of aniline (approximately 80%) was bound by strong binding forces that cannot be released by ethanol.

The addition of ultrasound significantly improved desorption efficiency, and now desorption was more effective with increasing ethanol concentrations. The high temperature and pressure generated by cavitation collapse caused more aniline molecules to detach from the PAC and enter the solution, and this was apparently promoted at higher ethanol concentrations. The desorption of aniline from the PAC in the presence of ethanol combined with ultrasound radiation was greater than the sum of the two separate treatments, indicating that ultrasound and ethanol produce a synergistic effect. Ethanol can reduce the tensile stress of the liquid and thus reduce the cavitation threshold and facilitate the generation of bubbles. The generation of more transient cavitation bubbles helps to produce easily the high-speed microjets and high-pressure shock waves of solvent as they collapse [35]. As the ethanol concentration increased, the tensile stress of the mixture was reduced in a concentration-dependent manner. High concentrations of ethanol also led to a decrease in polarity of the mixture, which increased attractive forces between aniline and ethanol. In addition, ethanol capture the primary radicals ($^{\bullet}OH$) to induce the formation and later accumulation of secondary free radicals ($^{\bullet}CH_2CH_2OH$), which beneficial for

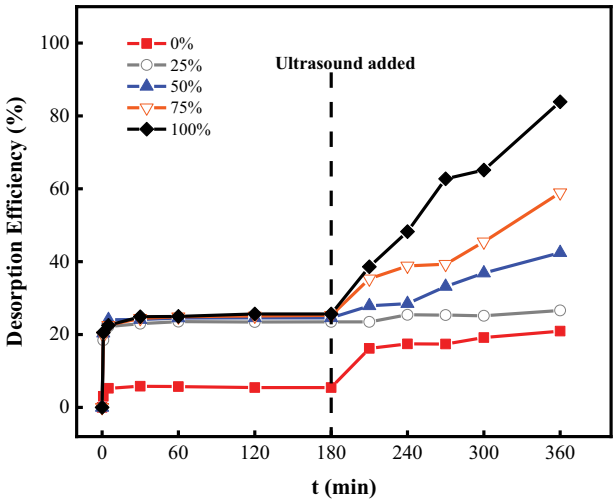

Fig. 4. Effect of alcohol added to the desorption solution without and with ultrasound treatment. Conditions of desorption: frequency = 40 kHz, power = 180 W, T = 298 K, pH = 7, the concentration of desorption solution = 0% (pure water) – 100% (v/v) ethanol.

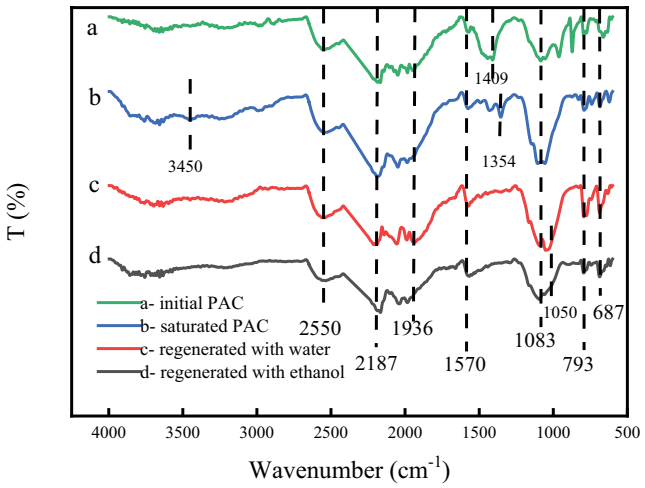

Fig. 5. FTIR spectra of PAC. Shown are curve (a) unused PAC, (b) aniline-saturated PAC, (c) used PAC after regeneration with water, and (d) used PAC after regeneration with ethanol.

the regeneration of GAC [36]. Therefore, adding ethanol can effectively improve the desorption efficiency. The synergistic, concentration-dependent effect of ethanol and ultrasound may be related to cavitation stimulation, decreased polarity and generated secondary free radicals.

3.3. Sonochemical effect on adsorbate and adsorbate during desorption

3.3.1. Chemical properties of PAC

In order to explore the surface properties of activated carbon during aniline adsorption and desorption, FTIR was carried out on the samples. The FTIR spectra of unused, saturated, water- recycled and ethanol-recycled PAC are shown in Fig. 5. These contain a number of bands observed in all four curves. The broadband at around 2,550 cm^{-1} was mainly attributed to NH^{+} stretching. The strong absorption band at 2,187 cm^{-1} corresponded to –C≡C– stretching. A double peak of strong absorption occurred at 1,083 cm^{-1} and this was assigned to C–OH stretching of alcohol. The band at 1,570 cm^{-1} and a high-intensity band at 1,409 cm^{-1} indicated the presence of –COO– on the surface of all samples and of unused PAC respectively. The absorption peaks observed in all four samples indicated that there were abundant functional groups such as –COOH, –C≡C– and C–OH on the surface of the PAC, irrespective of treatment.

After adsorption of aniline, the spectrum of the PAC changed. Compared to curve *a* new absorption peaks appeared in curve *b*. These included a band at 3,450 cm^{-1}, which was mainly assigned to the anti-symmetric stretching vibration of the aromatic primary amine present in aniline. The band at 1,354 cm^{-1} was ascribed to the C–N stretching of the aromatic primary amine of the adsorbate. Between 1,570 and 1,354 cm^{-1}, multiple absorption peaks appear, mainly caused by the skeleton vibration of the aromatic ring [37]. In the fingerprint region a band appeared around 740 cm^{-1}, indicating the existence of $–NH_2$ distorted vibration. These new absorption peaks were mainly caused by adsorbed aniline. In addition, the absorption intensity at 1,409 cm^{-1} decreased in curve *b*, indicating that carboxylic acid on the surface of PAC was linked to aniline functional groups.

Comparing curve *b* with curve *c*, the absorption peaks at 3,450 and 740 cm^{-1} disappeared as a result of desorption in water, while the intensity of absorption peaks at 793 and 687 cm^{-1} became stronger. The peak at 793 cm^{-1} represented the external bending vibration of C–H of a substituted benzene ring, and 687 cm^{-1} was caused by the vibration of carboxylate. Their presence indicated that intermediate products containing carboxylate were formed during ultrasound desorption in water. This may be the result of the degradation of pollutants on the surface of activated carbon directly by ultrasound, or the peaks may result from adsorption of degradation products in solution.

Compared with curve *b*, in curve *d* (desorption by ultrasound in ethanol) the bands at 3,450 cm^{-1}, and those between 1,570 and 1,354 cm^{-1} disappeared, as did the distorted vibration absorption band of $–NH_2$ in the fingerprint region, proving that ultrasound successfully desorbed aniline from the surface of PAC. Desorption in ethanol produced regenerated activated carbon with chemical properties closest to the original carbon. It indicated that regeneration in ethanol had little effect on the surface chemical properties of the PAC.

3.3.2. Structure of PAC before and after use and regeneration

Previous literature reported that the microjets and microstreams caused by the collapse of cavitation bubbles during ultrasound treatment present the main mechanism of activated carbon regeneration [38]. Under low-frequency ultrasonic treatment there were size limitations to the cavitation and corresponding microjets and microstreams, resulting in high-speed microjets and high-pressure shock waves generated by the cavitation bubble collapsed that mainly act on the surface and the mesopore of the carbon

[30]. Therefore, the surface area and pores of the PAC before and after ultrasonic irradiation were compared. The specific surface area, pore volume and pore diameter of unused, saturated, water-recycled and anhydrous ethanol-recycled carbon are shown in Table 3. After ultrasound radiation, the specific surface area of the PAC increased. Compared with saturated carbon, the specific surface area of PAC regenerated with pure water or with ethanol increased with 6.24% and 15.07% from 505.83 m^2/g, respectively. After ultrasonic treatment, the volume of the micro-pores hardly changed and remained around 0.04 cm^3/g, but the volume of mesopore increased, to sizes exceeding those of the unused carbon. These observations suggested that ultrasound irradiation expanded the mesopore of PAC.

Pore expansion was stronger under the synergy of ultrasound and ethanol. Compared with the water-recycled carbon, the total pore volume and mesopore volume of the ethanol-recycled carbon increased by 12.20% and 16.22%, respectively, and the average pore diameter also increased, by 2.94%. This indicated that microjets and microstreams produced by cavitation bubble collapse were more intense and more easily transmitted in ethanol, and the shock of the microjets or the microstreams could directly affect the surface of the PAC. Micropores provided most of the surface area where adsorption occurred, while mesopore was mainly distributed on the outer surface of PAC, providing passageways for absorbable molecules to reach the inner micropores more easily [9]. Since ultrasonic frequency negatively affected the diameter of cavitation bubbles as discussed above, due to the size limitations of the cavitation bubbles at low frequency the shock of the microjets or the microstreams most likely directly affected the surface of the PAC, rather than the inner micropores.

The surface of the PAC samples was also investigated by scanning electron microscopy. It can be clearly seen that the surface of the unused PAC was smooth (Fig. 6a). After adsorption of aniline, its surface showed many impurities (Fig. 6b). After ultrasonic regeneration in pure water, the impurities were removed, but the carbon surface was now less regular and slightly rough (Fig. 6c). After ultrasonic irradiation in the presence of ethanol, the surface of the carbon was more roughened, and many fractures were visible (Fig. 6d). This may be due to the high-speed microjets and high-pressure shock waves generated by cavitation bubbles acting on the surface structure of PAC that destroyed the surface structure of activated carbon. Strong cavitation in ethanol led to a higher desorption rate. High-speed microjets and high-pressure microstreams played an active role in the desorption process.

3.3.3. Chemical properties of aniline

During desorption only a portion of the aniline entered the solution, while the rest remains adsorbed on the PAC. As the concentration of aniline in the solution increased, the $^{\bullet}OH$ produced by ultrasonic cavitation had a higher probability to come into contact with aniline in solution. This may cause some of the aniline to degrade. It has been reported that using ultrasound to enhance the persulfate degradation of aniline and confirmed that its degradation was enhanced by ultrasonic treatment [4].

To investigate if any aniline in solution could be degraded under the ultrasound conditions used here, desorption of aniline in anhydrous ethanol and in pure water was mimicked in the absence of PAC, with a concentration of 50 mg/L aniline. Under ultrasound irradiation, the volatility and the hydrophobicity of a molecule determine where the degradation reaction occurs [39]. To determine the zones of the molecule where degradation occurred, *n*-butanol and acetic acid were added as scavengers of OH to the water. As short-chain alcohol, *n*-butanol can effectively remove cavitation bubbles in the gaseous and interfacial regions [40,41], while acetic acid reacts mainly with hydroxyl radicals in solution [42].

The degradation results are shown in Fig. 7. Using water as the solvent, the addition of *n*-butanol and acetic acid reduced the degradation efficiency from 17.2% to 6.6% and 16.0%, respectively. That means the degradation of aniline by ultrasound treatment was partly quenched with a stronger effect from *n*-butanol than from acetic acid. This suggested that most of the aniline was degraded by hydroxyl radical attack at the liquid-bubble interface. Degradation still occurred in the presence of the quenching agents. Since aniline is semi-volatile, the thermal reaction in the cavities will lead to aniline volatilization, and because of its hydrophobic character, the thermal reaction at the interface of cavitation bubbles may also be responsible for the decrease in soluble aniline.

There was hardly any degradation of aniline in ethanol due to the inhibitory effect of ethanol on hydroxyl radicals. Moreover, anhydrous ethanol is volatile. When stirred, the volatilization of the ethanol caused the solvent to decrease faster than the solute. Using ethanol as the solvent, the strong oxidation ability of hydroxyl radicals was inhibited.

Table 3
Specific surface area and pore analysis of PAC

PAC type	Specific surface area (m^2/g)			Pore volume (cm^3/g)			Average Pore size (nm)
	BET	*T*-Plot external surface area	*T*-Plot micropore surface area	Total volume	Micropore volume	Mesopore volume	
Unused	624.40	394.19	230.21	0.44	0.10	0.34	2.81
Saturated	505.83	106.85	398.98	0.38	0.04	0.34	3.01
Water-recycled	537.39	102.86	434.53	0.41	0.04	0.37	3.06
Ethanol-recycled	582.04	85.11	496.93	0.46	0.03	0.43	3.15

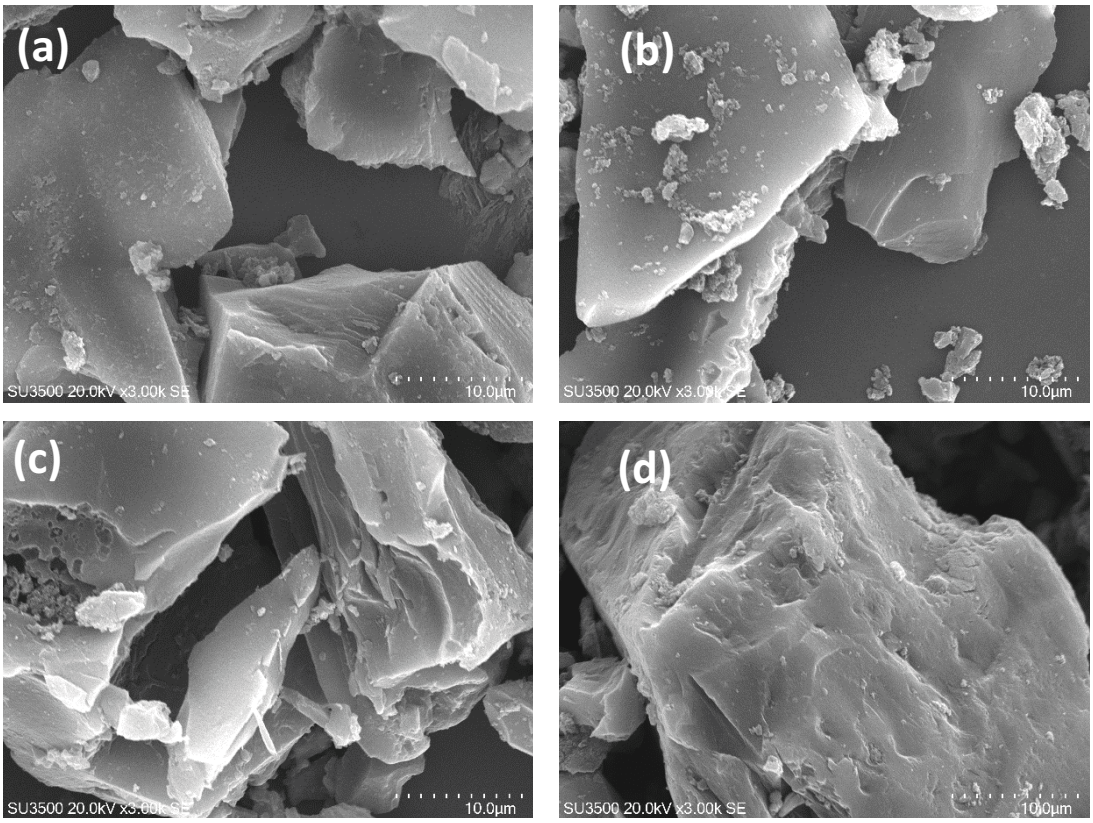

Fig. 6. SEM images of the (a) unused PAC, (b) after saturation with aniline, (c) following regeneration with water, and (d) after regenerated with anhydrous ethanol.

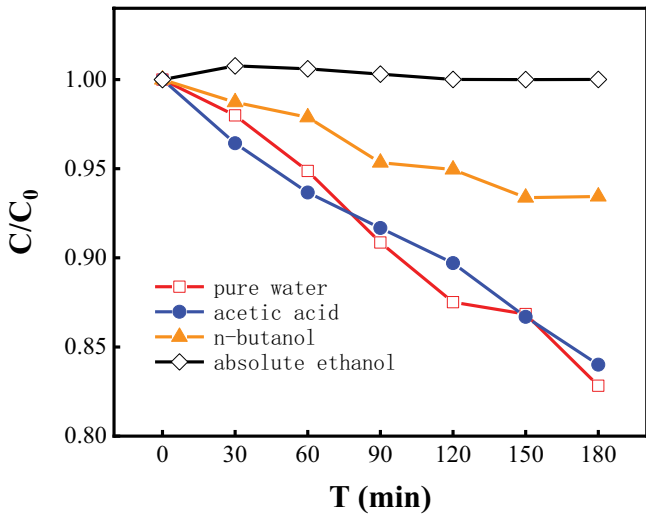

Fig. 7. Degradation by ultrasound treatment of aniline in water, in anhydrous ethanol, and in water with added radical scavengers *n*-butanol or acetic acid. Ultrasound was applied at 40 kHz and 180 W.

In order to further explore the effect of ultrasonic irradiation on aniline during desorption from PAC with water or ethanol, the liquid phase resulting from desorption experiments was analyzed by GC-MS.

The described mechanisms for aniline degradation results in two possible outcomes that are, symmetrical azo bond formation or formation of nitrobenzene [4]. In this study, only one product, azobenzene, was detected by GC-MS (Table A1). Formation of azobenzene may be enabled by iminobenzene radicals [43] that can form from aniline following an attack by OH, resulting in the loss of an electron. This iminobenzene radical was sensitive to substitution so that azobenzene can form by oxidation and head-to-head coupling through a two-electron process, the results are similar to previous studies [44,45]. However, the imine group was not further converted to nitrobenzene, and products such as phenol and benzoquinone were also not detected, indicating a limited ultrasonic oxidation ability. Fig. 8 shows the possible degradation pathway. No intermediate products were found in the degradation of aniline in ethanol, which indicated that ethanol inhibits aniline degradation. Combined with the changes of chemical properties of aniline and the physical structure of activated carbon during ultrasonic irradiation, it can be inferred that during desorption of ultrasound and ethanol, the synergistic effect had little relationship with the oxidation of adsorbate by hydroxyl radicals, but was mainly related to the high temperature and high pressure caused by cavitation bubble collapse.

4. Conclusion

The adsorption characteristics of aniline by PAC and its ultrasonic desorption efficiency and mechanism were studied.

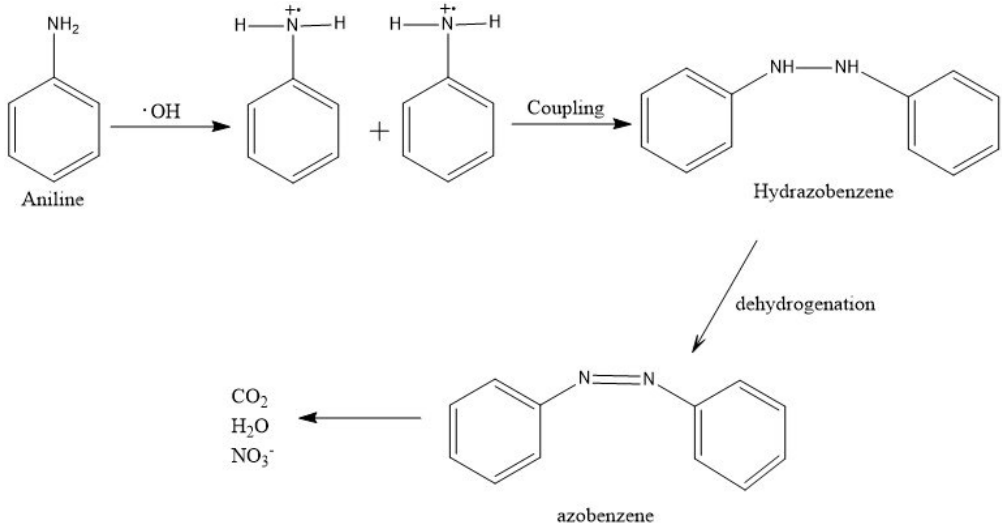

Fig. 8. Plausible reaction pathway of aniline degradation to form azobenzene in pure water under ultrasonic radiation.

The adsorption of aniline onto PAC followed the pseudo-second-order model and the Langmuir model. Desorption was most efficient at acidic pH, while the adsorption efficiency was the lowest. The optimal condition for desorption by ultrasound treatment was 180 W, with a frequency of 40 kHz at a pH of 3. The addition of ethanol during desorption produced a synergistic effect with ultrasound treatment, which greatly improved the desorption rate of aniline. The high-speed microjets and high-pressure microstreams generated by cavitation collapse mainly act on the surface and mesopore of PAC. Hydroxyl radicals produced by sonochemistry can degrade aniline in water to some extent, while the oxidation was inhibited when ethanol was used as the solvent.

Acknowledgements

The authors acknowledge the financial support of the National Natural Science Foundation of China (51778012). We would like to give our sincere thanks to the peer-reviewers for their suggestions.

References

[1] H. Tang, J. Li, Y. Bie, L. Zhou, J. Zhou, Photochemical removal of aniline in aqueous solutions: switching from photocatalytic degradation to photo-enhanced polymerization recovery, J. Hazard. Mater., 175 (2010) 977–984.
[2] F.Q. An, D. Zhang, X.X. Yue, G.L. Ou, J.F. Gao, T.P. Hu, Effective removal of anilines using porous activated carbon based on urea-formaldehyde resin, Korean J. Chem. Eng., 33 (2016) 576–581.
[3] G.Q. Wu, X. Zhang, H. Hui, J. Yan, Q.S. Zhang, J.L. Wan, Y. Dai, Adsorptive removal of aniline from aqueous solution by oxygen plasma irradiated bamboo-based activated carbon, Chem. Eng. J., 185–186 (2012) 201–210.
[4] S. Song, Z.Q. He, J.M. Chen, US/O_3 combination degradation of aniline in aqueous solution, Ultrason. Sonochem., 14 (2007) 84–88.
[5] F. Orshansky, N. Narkis, Characteristics of organics removal by PACT simultaneous adsorption and biodegradation, Water Res., 31 (1997) 0–398.
[6] Y. Han, X. Quan, S. Chen, H.M. Zhao, C. Cui, Y. Zhao, Electrochemically enhanced adsorption of aniline on activated carbon fibers, Sep. Purif. Technol., 50 (2006) 365–372.
[7] B. Kakavandi, A.J. Jonidi, R. Rezaei, S. Nasseri, A. Ameri, A. Esrafily, Synthesis and properties of Fe_3O_4-activated carbon magnetic nanoparticles for removal of aniline from aqueous solution: equilibrium, kinetic and thermodynamic studies, Iran. J. Environ. Health Sci. Eng., 10 (2013) 19.
[8] B. Pardo, N. Ferrer, J. Sempere, R.G. Olmos, A key parameter on the adsorption of diluted aniline solutions with activated carbons: the surface oxygen content, Chemosphere, 162 (2016) 181–188.
[9] J.L. Lim, M. Okada, Regeneration of granular activated carbon using ultrasound, Ultrason. Sonochem., 12 (2005) 277–282.
[10] X.H. Duan, C. Srinivasakannan, J.S. Liang, Process optimization of thermal regeneration of spent coal-based activated carbon using steam and application to methylene blue dye adsorption, J. Taiwan Inst. Chem. Eng., 45 (2014) 1618–1627.
[11] R.V. Mcquillan, G.W. Stevens, K.A. Mumford, The electrochemical regeneration of granular activated carbons: a review, J. Hazard. Mater., 355 (2018) 34–49.
[12] S.Y. Chen, H.C. Hsi, M.Y. Shih, Bioregeneration of spent mercury bearing sulfur-impregnated activated carbon adsorbent, Environ. Sci. Pollut. Res., 25 (2018) 5095–5104.
[13] D. Guo, Q. Shi, B. He, X. Yuan, Different solvents for the regeneration of the exhausted activated carbon used in the treatment of coking wastewater, J. Hazard. Mater., 186 (2011) 1788–1793.
[14] E. Yagmur, S. Turkoglu, A. Banford, Z. Aktas, The relative performance of microwave regenerated activated carbons on the removal of phenolic pollutants, J. Cleaner Prod., 149 (2017) 1109–1117.
[15] R.S. Juang, S.H. Lin, C.H. Cheng, Liquid-phase adsorption and desorption of phenol onto activated carbons with ultrasound, Ultrason. Sonochem., 13 (2006) 251–260.
[16] O. Hamdaoui, E. Naffrechoux, J. Suptil, C. Fachinger, Ultrasonic desorption of *p*-chlorophenol from granular activated carbon, Chem. Eng. J., 106 (2005) 153–161.
[17] Q. Hu, D.W. Gao, H. Pan, L. Han, P. Wang, Equilibrium and kinetics of aniline adsorption onto crosslinked sawdust-cyclodextrin polymers, RSC Adv., 4 (2014) 40071–40077.
[18] N. Wang, L. Zhu, M. Wang, D. Wang, H. Tang, Sono-enhanced degradation of dye pollutants with the use of H_2O_2 activated by Fe_3O_4 magnetic nanoparticles as peroxidase mimetic, Ultrason. Sonochem., 17 (2009) 78–83.
[19] M. Goel, H. Hongqiang, A.S. Mujumdar, M.B. Ray, Sonochemical decomposition of volatile and non-volatile organic

compounds—a comparative study, Water Res., 38 (2004) 0–4261.
[20] J.J. Yao, M.R. Hoffmann, N.Y. Gao, Z. Zhang, L. Li, Sonolytic degradation of dimethoate: kinetics, mechanisms and toxic intermediates controlling, Water Res., 45 (2011) 0–5894.
[21] A.D. Farmer, A.F. Collings, G.J. Jameson, Effect of ultrasound on surface cleaning of silica particles, Int. J. Miner. Process., 60 (2000) 101–113.
[22] W.S. Chen, C.P. Huang, Mineralization of aniline in aqueous solution by electro-activated persulfate oxidation enhanced with ultrasound, Chem. Eng. J., 266 (2015) 279–288.
[23] H. Al-Johani, M.A. Salam, Kinetics and thermodynamic study of aniline adsorption by multi-walled carbon nanotubes from aqueous solution, J. Colloid Interface Sci., 360 (2011) 760–767.
[24] V. Malgras, Q. Ji, Y. Kamachi, T. Mori, F.K. Shieh, K.C.W. Wu, K. Arige, Y. Yamauchi, Cheminform abstract: templated synthesis for nanoarchitectured porous materials, Bull. Chem. Soc. Jpn., 88 (2015) 1171–1200.
[25] H. Zheng, Y. Wang, Y. Zheng, H. Zhang, S. Liang, M. Long, Equilibrium, kinetic and thermodynamic studies on the sorption of 4-hydroxyphenol on Cr-bentonite, Chem. Eng. J., 143 (2008) 117–123.
[26] Q. Qin, J. Ma, K. Liu, Adsorption of nitrobenzene from aqueous solution by MCM-41, J. Colloid Interface Sci., 315 (2007) 80–86.
[27] M.R. Samarghandi, M. Zarrabi, M.N. Sepehr, A. Amrane, G.H. Safari, Application of acidic treated pumice as an adsorbent for the removal of azo dye from aqueous solutions: kinetic, equilibrium and thermodynamic studies, Iran. J. Environ. Health Sci. Eng., 9 (2012) 9.
[28] H. Nourmoradi, M. Avazpour, N. Ghasemian, M. Heidaric, K. Moradnejadid, F. Khodarahmia, M. Javaheria, F. Mohammadi Moghadame, Surfactant modified montmorillonite as a low cost adsorbent for 4-chlorophenol: equilibrium, kinetic and thermodynamic study, J. Taiwan Inst. Chem. Eng., 59 (2016) 244–251.
[29] X. Xing, C. Feng, Enhancing CO_2, desorption from crude oil by ultrasound, Ultrasonics, 84 (2018) 74–80.
[30] C. Liu, Y. Sun, D. Wang, Z. Sun, M. Chen, Z. Zhou, W. Chen, Performance and mechanism of low-frequency ultrasound to regenerate the biological activated carbon, Ultrason. Sonochem., 34 (2017) 142–153.
[31] M.A. Beckett, I. Hua, Impact of ultrasonic frequency on aqueous sonoluminescence and sonochemistry, J. Phys. Chem. A, 105 (2001) 3796–3802.
[32] N. Pokhrel, Vabbina, P. Kiran, Pala, Nezih, Sonochemistry: science and engineering, Ultrason. Sonochem., 29 (2016) 104–128.
[33] R. Hu, S. Dai, D. Shao, A. Alsaedi, B. Ahmad, X. Wang, Efficient removal of phenol and aniline from aqueous solutions using graphene oxide/polypyrrole composites, J. Mol. Liq., 203 (2015) 80–89.
[34] L. Zuo, W. Song, T. Shi, C. Lv, J. Yao, J. Liu, Y. Wang, Adsorption of aniline on template-synthesized porous carbons, Microporous Mesoporous Mater., 200 (2014) 174–181.
[35] O. Hamdaoui, E. Naffrechoux, L. Tifouti, C. Petrier, Effects of ultrasound on adsorption–desorption of *p*-chlorophenol on granular activated carbon, Ultrason. Sonochem., 10 (2003) 109–114.
[36] D. Feng, H. Tan, J.S.J.V. Deventer, Ultrasonic elution of gold from activated carbon, Miner. Eng., 16 (2003) 257–264.
[37] B. Ledesma, S. Román, A. Álvarez-Murillo, E. Sabio, C.M. González-García, Fundamental study on the thermal regeneration stages of exhausted activated carbons: kinetics, J. Therm. Anal. Calorim., 115 (2014) 537–543.
[38] Y. Yao, Enhancement of mass transfer by ultrasound: application to adsorbent regeneration and food drying/dehydration, Ultrason. Sonochem., 31 (2016) 512–531.
[39] I. Gültekin, N.H. Ince, Ultrasonic destruction of bisphenol-A: the operating parameters, Ultrason. Sonochem., 15 (2008) 524–529.
[40] S. Adityosulindro, L. Barthe, K. González-Labrada, U.J.J. Haza, H. Delmas, C. Julcour, Sonolysis and sono-Fenton oxidation for removal of ibuprofen in (waste) water, Ultrason. Sonochem., 39 (2017) 889–896.
[41] Q.P. Isariebel, J.L. Carine, J.H. Ulises-Javier, W. Anne-Marie, D. Henri, Sonolysis of levodopa and paracetamol in aqueous solutions, Ultrason. Sonochem., 16 (2009) 610–616.
[42] R. Xiao, D. Diaz-Rivera, Z. He, L.K. Weavers, Using pulsed wave ultrasound to evaluate the suitability of hydroxyl radical scavengers in sonochemical systems, Ultrason. Sonochem., 20 (2013) 990–996.
[43] A. Kumar, N. Mathur, Photocatalytic degradation of aniline at the interface of TiO_2 suspensions containing carbonate ions, J. Colloid Interface Sci., 300 (2006) 244–252.
[44] S. Laha, R.G. Luthy, Oxidation of aniline and other primary aromatic amines by manganese dioxide, Environ. Sci. Technol., 24 (1990) 363–373.
[45] L. Jiang, L. Liu, S. Xiao, J. Chen, Preparation of a novel manganese oxide-modified diatomite and its aniline removal mechanism from solution, Chem. Eng. J., 284 (2015) 609–619.

Appendix

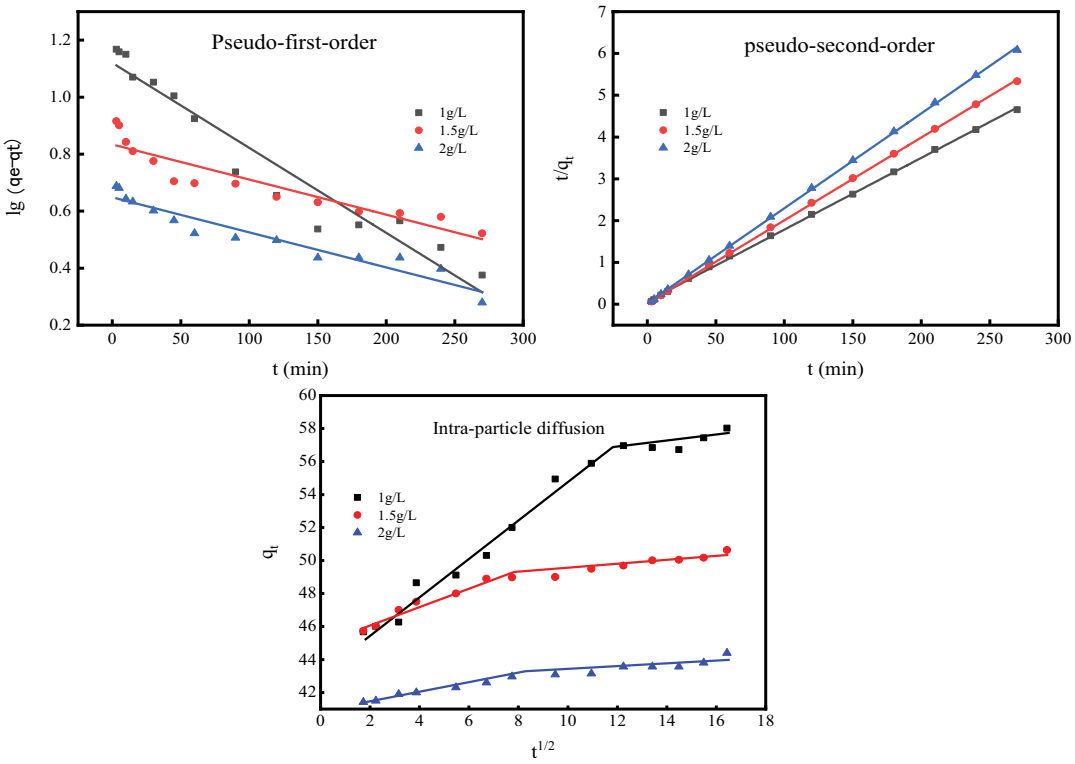

Fig. A1. Adsorption kinetics of the three fitting models.

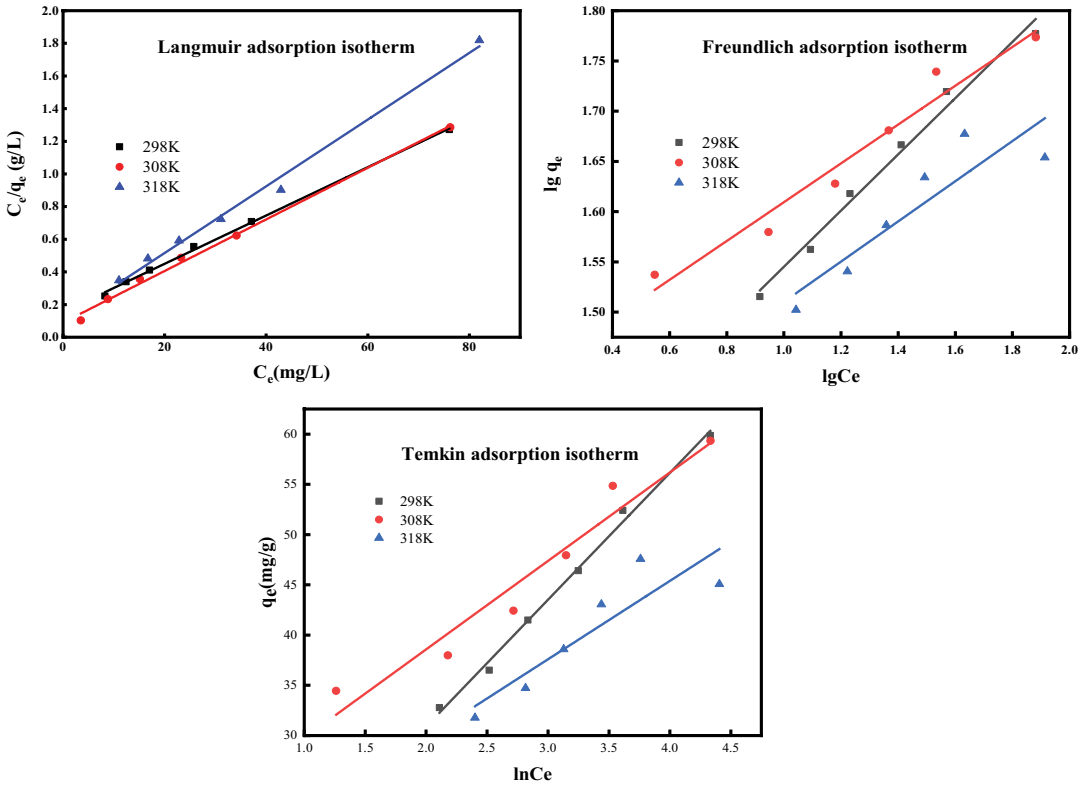

Fig. A2. Adsorption isotherms of aniline onto PAC.

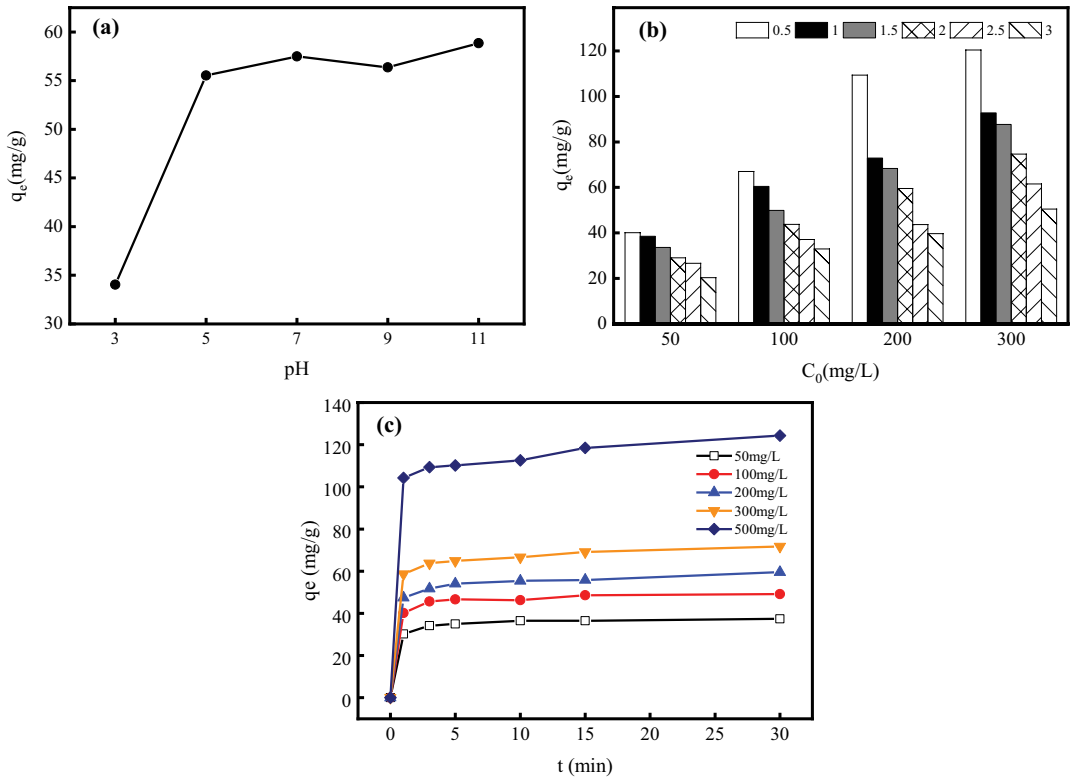

Fig. A3. Factors affecting the adsorption of aniline onto PAC: (a) effect of solution pH (condition: 1 g/L PAC; initial aniline concentration C_0 = 100 mg/L, t = 270 min, T = 298 K), (b) effect of variable initial aniline concentration (C_0) and PAC doses (shaded bars) and (c) effect of contact time for five initial aniline concentrations.

Table A1
Compositions of degradation intermediates identified by GC-MS

Component	m/z (relative abundance, %)
Azobenzene	50 (4.25), 51 (25.84), 57 (4.36), 77 (100), 78 (7.61), 95 (4.58), 105 (24.27), 152 (5.66), 182 (18.35)